Identification of Phosphorylation-Induced Changes in Vimentin Intermediate Filaments by Site-Directed Spin Labeling and Electron Paramagnetic Resonance[†]

Josh T. Pittenger,[‡] John F. Hess,[‡] Madhu S. Budamagunta,[§] John C. Voss,[§] and Paul G. FitzGerald*[,‡]

Department of Cell Biology and Human Anatomy and Department of Biochemistry and Molecular Medicine, School of Medicine, University of California, Davis, California 95616

Received June 17, 2008; Revised Manuscript Received August 18, 2008

ABSTRACT: Phosphorylation drives the disassembly of the vimentin intermediate filament (IF) cytoskeleton at mitosis. Chromatographic analysis has suggested that phosphorylation produces a soluble vimentin tetramer, but little has been determined about the structural changes that are caused by phosphorylation or the structure of the resulting tetramer. In this study, site-directed spin labeling and electron paramagnetic resonance (SDSL-EPR) were used to examine the structural changes resulting from protein kinase A phosphorylation of vimentin IFs in vitro. EPR spectra suggest that the tetrameric species resulting from phosphorylation is the A11 configuration. EPR spectra also establish that the greatest degree of structural change was found in the linker 2 and the C-terminal half of the rod domain, despite the fact that most phosphorylation occurs in the N-terminal head domain. The phosphorylation-induced changes notably affected the proposed "trigger sequences" located in the linker 2 region, which have been hypothesized to mediate the induction of coiled-coil formation. These data are the first to document specific changes in IF structure resulting from a physiologic regulatory mechanism and provide further evidence, also generated by SDSL-EPR, that the linker regions play a key role in IF structure and regulation of assembly/disassembly.

The intermediate filament (IF)[1] protein family is the largest of the three major classes of cytoskeleton proteins and consists of more than 65 human IF genes (*1*). IF proteins exhibit considerable primary sequence variation but share a well-conserved predicted secondary structure that consists of an α-helical central rod domain flanked by head and tail domains that are highly variable in both size and sequence (*2*−*4*). The rod domain is approximately 310 amino acids in length and is often described as consisting of four α-helical "coil" regions (1A, 1B, 2A, and 2B), separated by three, nonhelical "linker" regions (L1, L12, and L2) (*5, 6*) (see schematic in Figure 1).

IF protein expression varies by cell type as well as the state of development/differentiation of the cell (reviewed (*7*)). The best known functions of IF proteins include protection against mechanical and metabolic stresses, but IF proteins have been implicated in a wide range of cellular functions including cell signaling, stress responses, and apoptosis (reviewed (*8*)). The numerous functions associated with IFs suggest that cellular regulatory mechanisms controlling IF characteristics such as assembly/disassembly must be well established. One such IF regulatory mechanism is phosphorylation.

Phosphorylation of IF proteins was first described in the late 1970s. Rapid turnover of IF phosphates during mitosis of amnion cells was correlated with structural changes in IF networks during this phase of the cell cycle, suggesting that phosphorylation of IFs might serve a possible regulatory role in cell cycle-dependent IF assembly/disassembly (*9, 10*). This hypothesis has been supported by direct evidence of phosphorylation as a regulatory mechanism for vimentin IF disassembly in vitro (*11*). Many subsequent studies have shown that nearly all IFs serve as cellular kinase phosphorylation targets (reviewed (*12*)). The list of regulatory functions conferred by IF phosphorylation is still growing, but filament organization, solubility, subcellular compartmentalization, expression, turnover, and susceptibility to stress have all been observed (*13*−*15*). The abundance of IF protein in a cell, combined with numerous phosphorylation sites per IF molecule, makes IF proteins among the most abundant cellular phosphoproteins (reviewed *16, 17*).

Neither the IF protein nor the IF has been successfully crystallized, though recent advances in achieving crystal structures of IF fragments have been reported (*18, 19*). For this reason, the complete structure of the IF remains unknown, as do changes that are induced in IF structure by phosphorylation. Phosphorylation of intact vimentin filaments in vitro leads to a characteristic disassembly into soluble subunits that have previously been classified as tetramers or higher order oligomers (*20*) on the basis of chromatographic behavior (*21*). Cross-linking data supporting the hypothesis

[†] Supported by grants from the National Institutes of Health, EY017575 (to P.G.F.), P30 EY012576, and AG029246 (to J.C.V.). This work was conducted in a facility constructed with support from Research Facilities Improvement Program Grant C06 RR-12088-01 from the National Center for Research Resources, National Institutes of Health.

* Corresponding author. Phone: 530-752-7130. Fax: 530-752-8520. E-mail: pgfitzgerald@ucdavis.edu.

[‡] Department of Cell Biology and Human Anatomy, University of California.

[§] Department of Biochemistry and Molecular Medicine, University of California.

[1] Abbreviations: IF, intermediate filament(s); SDSL, site-directed spin labeling; EPR, electron paramagnetic resonance; MSL, maleimide spin label; MTSL, methanethiosulfonate spin label.

10.1021/bi801137m CCC: $40.75
Published on Web 09/20/2008

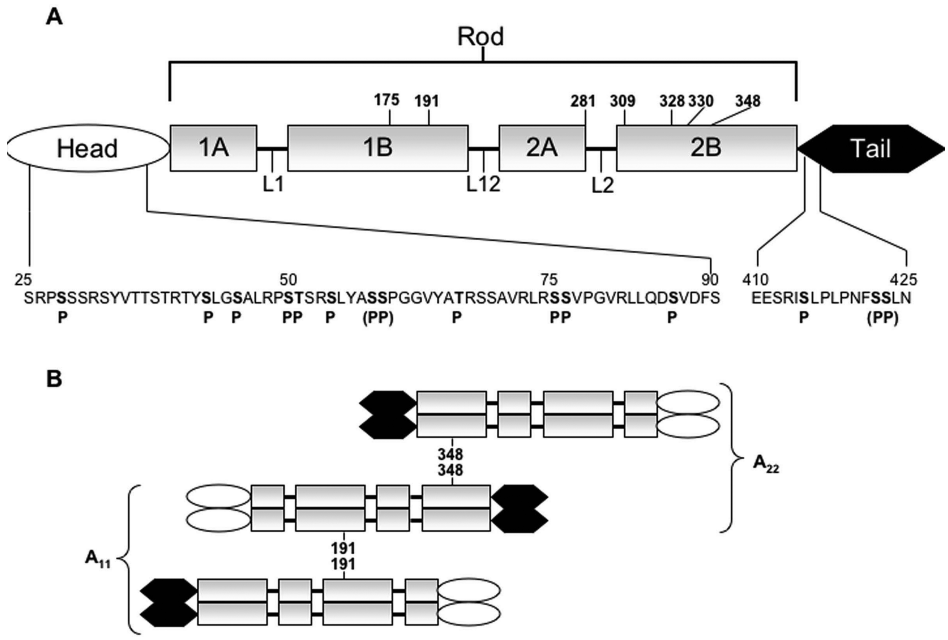

FIGURE 1: (A) Schematic depiction of the vimentin molecule with variable head/tail regions and a rod domain punctuated by linker regions. Cysteine mutants spin labeled for EPR are listed above the molecule; phosphorylation sites identified in this study are listed below. (B) Schematic depiction of A11 and A22 alignments of the vimentin tetramer and the relative proximity of positions 191 and 348.

that tetramers are the end stage breakdown product of phosphorylated filaments have been presented (*20*).

Recent evidence suggests that phosphorylation-specific conformational changes of individual IF proteins may also be occurring below the tetramer level. Studies using K8 antibodies show masking of an upstream epitope site caused by phosphorylation at a specific residue downstream. The epitope recognized is distant from known phosphorylation sites, which suggests structural changes of individual IF proteins below the dimer level (*22*). Theoretically, monomer- or dimer-specific structural changes by phosphorylation could play a large role in IF regulation by masking or unmasking IF-associated protein binding sites driving cellular or cell-cycle-specific functions.

Several in vitro and in vivo studies have identified numerous phosphorylation sites in the highly variable head and tail domains of IF proteins but none in the rod (*23, 24*). Vimentin contains approximately 20 in vivo phosphorylation sites, predominantly in the head domain (*20, 25*−*27*). Studies have also shown vimentin may serve as a phosphorylation target for a number of kinases in vitro that may or may not have IF regulatory roles in vivo. Yet, in vitro phosphorylation of vimentin has been shown to mimic interphase-specific phosphorylation sites as well as produce disassociated vimentin oligomers similar to those released during in vivo phosphorylation (*20*). At least one study reported the assembly competence of phosphorylated vimentin (*28*).

We have utilized site-directed spin labeling (SDSL) and electron paramagnetic resonance (EPR) to elucidate IF structural characteristics in vimentin (reviewed (*29*)). In concert with cross-linking data, SDSL-EPR has yielded valuable information on secondary, tertiary, and quaternary structure of IF proteins (*30*−*35*). More specifically, SDSL-EPR has been able to define specific intermolecular interactions between IF monomers in intact dimers and between dimers in filaments, as well as to monitor changes in local structure that occur during assembly, thermal denaturation, and as a result of known disease-causing mutations (*28*−*35*). In this study, SDSL-EPR was used to examine structural changes occurring as a result of protein kinase A (PKA) phosphorylation of vimentin IFs in vitro.

EXPERIMENTAL PROCEDURES

Vimentin mutation, characterization, cloning, expression, purification, and spin labeling were described in detail in previous reports (*32, 33*). In brief, a spin label is ultimately attached to a cysteine residue that is targeted to a specific site in the vimentin protein. Following conversion of the lone endogenous cysteine to serine (C328S), single cysteine codons were introduced into the vimentin expression construct (generously provided by Dr. Roy Quinlan, University of Durham, Durham, U.K.) using the Stratagene QuikChange kit (Stratagene, La Jolla, CA). Sequence changes were verified by DNA sequencing. Mutant vimentin was produced by bacterial expression using a pT7 vector and arabinose-inducible BL21(DE3) cells (Invitrogen, Carlsbad, CA). Inclusion bodies were purified from bacterial cell pellets using high/low salt washes and chromatography. Fractions were run and analyzed by 10% SDS−PAGE. Peak protein fractions were pooled into a primary stock.

Spin labeling was accomplished by incubation of the purified vimentin in 100 μM TCEP (Molecular Probes, Eugene, OR) followed by 500 μM 3-malemidoproxyl (253375; Sigma Aldrich, St. Louis, MO). The unincorporated spin label was removed by CM-Sepharose chromatography using an Amersham Pharmacia FPLC. Labeled proteins were stored long term at −80 °C.

Filament assembly of mutant vimentin protein (~2 mg/mL) was performed as a single step dialysis similar to previous reports although the dialysis buffer was altered to kinase reaction buffer (*20*). In short, mutant vimentin proteins were dialyzed overnight in 20 mM Hepes, 60 mM NaCl, 2 mM $MgCl_2$, and 6 mM EGTA (filament assembly buffer) at room temperature. For every spin-labeled mutant, filament

Table 1: Phosphorylated Residues Identified by Mass Spectroscopy of Vimentin 328C Following Kinase plus ATP Treatment[a]

peptide	phosphopeptide sequence[b]	phosphorylated residue	previously identified[c]
1	MFGGPGTASRP<u>S</u>SSR	Ser28	yes
2	TY<u>S</u>LGSALR	Ser42	yes
3	TYSLG<u>S</u>ALRPSTSR	Ser45	yes
4	SLGSALRP<u>S</u>TSR	Ser50	yes
5	TY<u>S</u>LGSALRPSTSRSLYA(<u>SS</u>)PGGVYATR	Thr51, Ser58, or Ser59	no, yes (59)
6	<u>S</u>LYASSPGGVYATR	Ser54	yes
8	SLYASSPGGVYA<u>T</u>RSSAVR	Thr66	no
9	LR<u>SS</u>VPGVR	Ser75, Ser76	yes, yes
10	LLQD<u>S</u>VDFSLADAINTEFK	Ser86	yes
11	LLEGEESRI<u>S</u>LPLPNFSSLNLR	Ser415	no
12	ISLPLPNF(<u>SS</u>)LNLR	Ser422 or Ser423	yes (422)

[a] Peptide number, tryptic peptide sequence, and phosphorylation position are given in columns 1−3, respectively. Column 4 describes whether the position has been previously identified in in vitro or in vivo studies. [b] Additional phosphopeptides recovered with overlapping phosphorylation sites have been omitted. [c] Previously identified vimentin phosphorylation sites in vivo and in vitro.

assembly competence was assessed by electron microscopy of negatively stained 10 μL samples removed from the dialysis reaction and stained with 1% uranyl acetate on Formvar-coated carbon grids with a Phillips CM-120 electron microscope operated at 80 kV acceleration voltage. Volumes (20 μL) of vimentin filaments were incubated for 3 h at 30 °C with either (a) 10 μL of assembly buffer (control), (b) 5 μL of 10 mM ATP and 5 μL of assembly buffer (ATP only), (c) 5 μL (1.7 units/μL) of protein kinase A (PKA) catalytic subunit from bovine heart (Sigma Aldrich) and 5 μL of assembly buffer (kinase only), or (d) 5 μL of 10 mM ATP and 5 μL (1.7 units/μL) of kinase (kinase ATP). Following treatment of the vimentin filament samples, 5 μL aliquots were reimaged by electron microscopy and alternatively used for mass spectrometry and EPR. Experimental and control samples were processed simultaneously to minimize sample-to-sample variability.

Control and kinase ATP-treated 328S samples, approximately 60 μg, were run on 10% SDS−PAGE. Protein bands of interest were excised from the SDS−PAGE gel using a sterile blade. The protein bands were submitted to the Genome Center Proteomics Core at the University of California, Davis, for mass spectrometry (LC/MS/MS) based protein identification and phosphopeptide mapping. Briefly, proteins were reduced and alkylated according to previously described procedures (*36*) and digested with sequencing grade trypsin per the manufacturer's recommendations (Promega, Madison, WI). Liquid chromatography tandem mass spectrometry (LC/MS/MS) protein identification was performed using a Waters Nano-Acquity UPLC (Milford, MA) coupled to a hybrid linear ion trap Fourier transform mass spectrometer (LTQ-FT) (Thermo-Fisher, San Jose, CA) through an ADVANCE Plug and Play nanospray source (Michrom Bioresources, Auburn, CA). Peptides were loaded on a Waters UPLC symmetry C18 180 μm × 20 mm peptide trap at a loading rate of 15 μL/min. Peptides were then eluted from the trap and separated by a nanoscale 100 μm × 15 cm Waters C18 1.7 μm BEH UPLC column. Peptides were eluted using a 70 min 2−80% gradient of buffer B (buffer A = 0.1% formic acid; buffer B = 95% acetonitrile and 0.1% formic acid). The top four ions in each survey scan in the FT (100000 resolution) were subjected to automatic low-energy CID in the linear ion trap, and the resulting uninterpreted MS/MS spectra were searched against the vimentin protein sequence using SEQUEST (Thermo-Fisher, San Jose, CA) and Modiro PTM explorer (Protagen, Dortmund Germany). Peptide identifications were considered potentially correct for SEQUEST for Xcorrs >1.5 for +1 charges, >2.0 for +2 charges, and >2.5 for +3 charges and Modiro significance scores greater than 90%. All spectra found to be potentially phosphorylated were manually verified to confirm the modification.

EPR was conducted on a JEOL X-band spectrometer equipped with a loop gap resonator. Approximately 5 μL of each treated sample was placed in a sealed quartz capillary tube. Spectra were acquired at 20−22 °C with a single 120 s scan over 100 G at a microwave power of 4 mW and a modulation amplitude (0.125 mT) optimized to the natural line width of the attached nitroxide. Spectra were normalized to the same number of spins according to their integrated intensities. To improve the fidelity of the calculation, double integration of each sample was performed following its solubilization in 2% SDS.

RESULTS

Figure 1A presents a schematic of predicted IF protein structure as a reference for subsequent discussion. The coiled-coil motif is an α helix that exhibits a heptad repeat pattern, where the *a* and *d* positions of the heptad are dominated by hydrophobic residues. Because of the backbone coiling, the *a* and *d* residues end up along one surface of the α helix, producing a hydrophobic "stripe" along that side of the helix, mediating the dimerization process. The fundamental building block of all IFs is an in-register, in-parallel dimer, resulting from coiled-coil formation by the central rod domains. IF dimers subsequently assemble into antiparallel tetramers, named for the rod domains that overlap. The A11 (overlapping in rod domain 1) and A22 (overlapping in rod domain 2) configurations are shown, centered on residues 191 and 348, which have been shown to be the midpoints of overlap (Figure 1B) (*32, 33, 35*).

The spin labels we employ are attached at cysteine residues. Thus, the first step in our studies was to remove the single endogenous cysteine in vimentin, creating the cysteine-free vimentin construct (C328S). To identify PKA phosphorylation sites on vimentin C328S, in vitro phosphorylated and nonphosphorylated vimentin samples were submitted to the UCD Mass Spectroscopy facility. Tandem mass spectrometry identified 13 peptides with S/T phosphorylations (Figure 1A, Table 1).The exact location of 11 of 13 phosphorylated amino acids could be determined by the MS/MS data. For the remaining 2, the MS/MS data were not conclusive, and the exact site of phosphorylation could

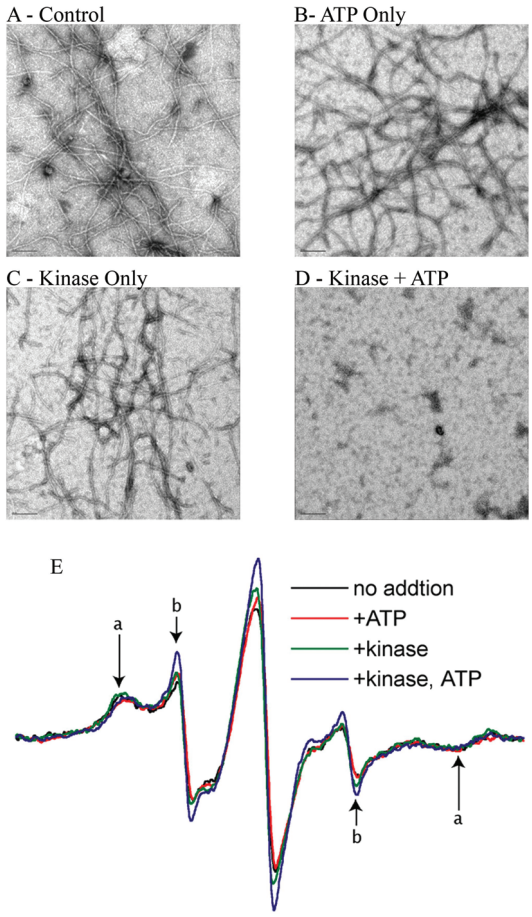

FIGURE 2: (A−D) Electron microscope images of vimentin IFs spin labeled at position 309. (A) No treatment. (B) ATP only treatment. (C) Kinase only treatment. (D) Kinase and ATP treatment. (E) Normalized EPR spectra of vimentin spin labeled at position 309 following the indicated treatments. The amplitude of each spectrum is normalized to the same number of spins. Arrows labeled a and b indicate components of the spectra discussed in the text.

not be determined. In concordance with published data, all identified phosphorylation sites were located in either the head or tail domains of the vimentin molecule (Figure 1A).

Of the identified phosphorylation sites in this experiment, 10 of 13 sites had previously been identified (in vitro or in vivo) as phosphorylation sites in vimentin (Table 1).

Following the identification of phosphorylation sites by mass spectroscopy, we used EPR to probe for structural changes in the vimentin IF occurring as a result of phosphorylation. Several different mutant proteins, each containing a single cysteine, were produced by bacterial expression, purified by chromatography, and spin labeled as previously described (*30*−*33*). Spin-labeled vimentin mutants were assembled into IFs by overnight dialysis against kinase reaction buffer (see Experimental Procedures). The presence of IFs was verified by electron microscopy. Intact vimentin IFs were then treated with (a) a buffer control, (b) ATP control, (c) kinase control, or (d) kinase in combination with ATP. As assessed by electron microscopy (Figure 2), samples treated with the various controls contained normal IFs (Figure 2A−C), whereas the sample treated with kinase plus ATP showed no filaments, verifying that the in vitro phosphorylation resulted in filament disassembly (Figure 2D). Aliquots of each treated sample were also subjected to EPR analysis. The control experiments, with additions of ATP alone, or

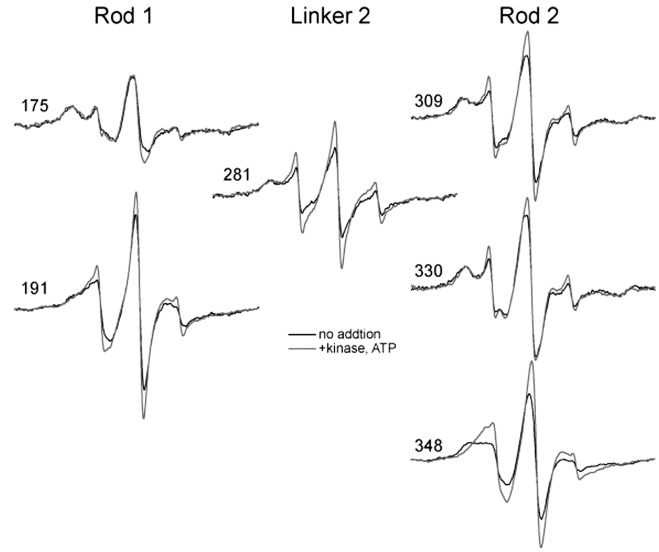

FIGURE 3: Normalized EPR spectra for vimentin mutants observed. For each indicated position, the black trace is the buffer control; the gray trace is the kinase plus ATP experimental sample.

kinase alone did not dissociate filaments and had little impact on the spectra (Figure 2E).

Note that previous studies employed the methanethiosulfonate spin label (MTSSL) which is attached to cysteine via a disulfide linkage (*30*−*33*). Reaction conditions for the PKA used in these experiments prevented the use of this spin label; DTT in the reaction would have released the spin label from the vimentin protein. We therefore employed the maleimide spin label (MSL) which was attached by alkylation of the targeted thiol. The spectrum of vimentin filaments containing the MSL spin label attached to position 309 reflects the predicted tight packing of the *a* position of the coiled-coil heptad. Steric constraints inhibit spin-label mobility, generating the clearly defined broad peaks at the hyperfine extrema (arrows labeled a in Figure 2E). However, in contrast to MTSSL-labeled 309C (*33*), 5−10% of the attached MSL spins display greater motional freedom, consistent with the notion that the larger MSL is less efficient in accommodating a tightly packed environment (arrows labeled b in Figure 2E) (*37*). As compared to the MTSSL label, less efficient packing of the MSL probe can also account for the attenuated level of dipolar broadening in its spectra when sites in close proximity (e.g., a/d positions) are examined.

In order to identify structural changes that occur as a result of kinase-induced filament disassembly, we placed spin labels at selected sites, each of which reported on structure at known locations. First, to determine if vimentin dimers remained intact following phosphorylation, we placed spin labels at a positions in the coiled-coil heptad in both rod 1B and rod 2B. These residues report on the monomer−monomer interactions that mediate coiled-coil dimerization (positions 175, 309, and 330). As seen in Figure 3, the spectra from vimentin spin labeled at position 175 is essentially unchanged by phosphorylation (black line, pre-kinase; gray line, post-kinase). This indicates no significant change in the structure of the vimentin near position 175 or, interpreted more generally, rod 1B. EPR spectra from positions within rod 2B, however, reveal a detectable difference between pre- and post-kinase spectra. When vimentin containing the spin label at position 309 or 330 was phosphorylated, the EPR spectra

reflected a small increase in the fraction of more mobile side chains. This change may arise from partial loosening of the coiled-coil association in a small fraction of the core dimer species. Alternatively, this may simply reflect an increase in the mobility of the weakly immobilized MSL labels due to the loss of contact with neighboring dimers induced by the phosphorylation. Regardless, the population of strongly immobilized side chains arising from the coiled-coil association remains largely intact at both positions following phosphorylation. Thus, while phosphorylation results in filament disassembly, we conclude it does not result in the dissociation of the coiled-coil dimer.

We previously reported the unexpected finding that linker 2 was a highly structured region with most positions showing a moderate to large level of dipolar coupling between labels within the in-parallel dimer (*30*). To explore whether phosphorylation affected linker 2 structure, we studied the impact of phosphorylation on vimentin constructs bearing a spin label at residue 281, a site within the linker 2 domain, between rod 2A and rod 2B (see Figure 1). Pre- and post-kinase spectra from position 281 (see Figure 3) reveal changes similar in nature, but greater in magnitude, to those from positions 309 and 330. Thus, it is also likely that the increased amplitude of the position 281 spectrum upon phosphorylation results from a loss of dipolar broadening as well as increased side chain flexibility. Interestingly, the linker 2 region is removed from any known phosphorylation sites (Figure 1). In particular, the substantial change at position 281 is noteworthy since linker 2 is locked into a definitive structure early in vimentin IF assembly and displays resistance to denaturation by heat or urea (*30*). Thus, perturbation of linker 2 structure may represent a critical conformational signal that directs the state of assembly in IFs.

In order to explore the impact of phosphorylation on dimer−dimer interactions, we placed spin labels at residues 191 and 348. These sites are non-a,d positions within the rod domain that reside on the "outer" surface of the coiled-coil dimer. As such, they report on interactions between the two dimers. We have shown in previous studies that positions 191 and 348 are the midpoints of the A11 and A22 tetramer alignments, respectively (*32, 33*). Thus spin labels at these residues will report on the status of the A11 and A22 interactions. Phosphorylation of vimentin IF produces a change in the EPR spectra of both positions 191 and 348. The postphosphorylation spectrum from spin-labeled position 191 is the same general line shape with greater amplitude, when compared to the control spectrum (Figure 3), indicating greater motional freedom from the spin-labeled side chain. Since the mobility and dipolar coupling of spin labels at position 191 are markers for the A11 alignment, this change reflects either an increase in the flexibility of the protein chains in the A11 tetramer (as compared to the intact IF) or a decrease in vimentin oligomers arranged in this alignment. Our interpretation is that the change in the spectra at position 191 is a result of increased flexibility.

The effect of phosphorylation on the spectrum of spin-labeled positios 348 vimentin is much more dramatic (Figure 3), with a substantial change in both the spectral amplitude and the shape of the splittings following filament phosphorylation. Since residue 348 is an *e* position within the coiled-coil heptad repeat of rod domain 2, its side chain projects outward on the surface of the core dimer unit. Earlier studies (*33*) have shown that the dipolar broadening apparent in spectra from labels attached to position 348 arises from the magnetic interaction between labels of adjacent coiled-coil dimers, establishing position 348 as a marker for the A22 alignment in filament assembly. In phosphorylated vimentin, the loss of the broad spectral features is consistent with a reduced contact between dimers and/or an increase in the distance between labels that correspond to the A22 alignment that is absent. However, since a narrower line shape is predicted for both increased side chain mobility (with a reduction in quaternary contact) and reduced dipolar coupling (with disruption of the A22 alignment), the effect of phosphorylation on the EPR spectrum of vimentin containing spin labels at position 348 was measured in the absence of molecular motion (−100 °C; Figure 4). In frozen spectra, a semiquantitative measure of the dipolar broadening can be obtained from the ratio of d_1/d (see Figure 4), where the magnitude of this ratio reflects the proximity of nitroxide labels within the range of 1−2 nm. The frozen spectra of vimentin with spin labels attached to position 348 show moderate dipolar broadening, with a d_1/d value of 0.44 (*38, 39*). In agreement with previous deconvolution of dipolar splittings in the solution spectrum (*33*), this value indicates an average interspin distance of ∼1.5 nm. In contrast, phospohorylated vimentin displays no appreciable broadening ($d_1/d = 0.33$), indicating spins are separated by at least 2 nm. This suggests that the filament disassembly induced by phosphorylation results in separation of the A22 dimer but not the A11 dimer.

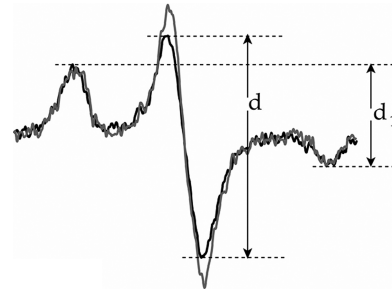

FIGURE 4: EPR spectra of frozen vimentin containing a spin-labeled side chain at position 348. The spectrum of phosphorylated vimentin is shown by the gray line, with control vimentin shown by the black trace. The extent of broadening is revealed by the qualitative parameter d_1/d, which is larger for labels experiencing greater dipolar interaction.

DISCUSSION

Several lines of evidence support the existence of stable tetramers of IF proteins under physiologic conditions: the soluble fraction of vimentin in a cell (*21*), the stable species formed following phosphorylation (*20*), and the stable species formed in solution following deletion of the head domain (*40, 41*). The characterization of these species as tetramers was based on sedimentation rates in a centrifugal field and the apparent molecular weight of cross-linked protein species electrophoresed on SDS−PA gels. However, in all but one of these cases, the identity of the tetramer was unspecified. The exception is the characterization of the assembly of headless vimentin by Mucke et al., which identified a headless vimentin tetramer as an A22 arrangement (*42*). We report here direct evidence that the A11 dimer−dimer

interaction is largely unchanged by phosphorylation, while the A22 interaction appears to be completely disrupted. This would suggest that the sole remaining tetrameric species is the one centered on the A11 interaction. The apparent contrast between our data identifying the A11 tetramer as first formed and most stable and the existence of headless A22 stable tetramers must be partially or completely explained by the head deletion used in that report.

In addition to these in vitro analyses, it has also been demonstrated that certain IF mutants, which are unable to assemble in vitro, are able to incorporate into existing IF networks (*40, 43*). Following the identification of the soluble tetrameric subunit of vimentin, the possibility of exchange of subunits into and out of assembled IFs was hypothesized (*21*). Evidence to support subunit exchange in intact IFs has been provided by photobleaching experiments and observing fluorescently tagged molecules (*44*). Our data indicate that phosphorylation produces A11 tetramers, and thus it seems likely that A11 tetramers are the soluble cellular vimentin subunit structure, suggesting A11 tetramers have the ability to exchange in and out of intact IFs. Taken together, it seems likely that a mutant able to form A11 tetramers but unable to assemble further in vitro would be able to integrate into existing IFs.

Existing evidence suggested that phosphorylation would not be expected to disrupt the vimentin monomer−monomer interaction: (a) phosphorylation induces the formation of tetramers and not monomers, and (b) phosphorylation sites are absent from the rod domain. For these reasons, we expected little to no change in spectra from spin labels placed at a,d positions in the coiled-coil domains. This proved to be the case for position 175 in rod 1B. However, spectra from residues 281, 309, and 330, which are from linker 2 and rod 2B, show some differences in spin-label behavior as a result of phosphorylation. For example, there is a clear increase in the fraction of the mobile component at residue 309, and at other sites as well, though to a lesser extent. Since residue 309 occupies an a position within the heptad repeat (i.e., at the interface of the coiled coil), one effect of phosphorylation is to decrease the fraction of side chains that are tightly packed in the interface. A second, more mobile component can also be seen with the MTSSL label attached to position 309 (*33*), though its amplitude is much smaller than the MSL label. The more prominent population of mobile species with MSL is consistent with other findings (*37*), with this behavior attributed to a diminished ability to pack in tight environments (due to its longer length and volume) and its lacking the backbone interactions favored by MTSSL (*45*). It is of interest to note that the spectrum of MSL-labeled 309 is identical whether the vimentin exists as intact filaments or protofilaments assembled at low ionic strength (which are thought to be comprised of two associated coiled-coil dimers; not shown). Thus, the amplitude of the mobile species does not depend on the stage of assembly beyond the tetramer stage, suggesting phosphorylation induces backbone perturbations that shift the equilibrium between these two rotamers of the spin label (mobile and immobile). However, even in the phosphorylated state, the fraction of the mobile labels represents a minor species.

Our subsequent study of the impact of phosphorylation on dimer−dimer interactions provides additional insights for this observation. We showed that the A11 tetrameric species survived phosphorylation, while the A22 did not. It is likely that intrinsic rigidity of the coiled coil is further enhanced by lateral interactions between dimers in higher order structures. The A22 tetramer which includes the linker 2 and rod 2B domains is disrupted by phosphorylation, and presumably, by virtue of the lack of stabilizing A22 protein contacts, more flexibility is permitted at positions 281, 309, and 330. Thus dimer−dimer stabilization is lost for rod 2 upon phosphorylation, but not for rod 1, creating an opportunity for greater spin-label motional freedom in rod 2 after phosphorylation. Thus a more extensive sampling of sites within vimentin will be very useful toward elucidating the effect of phosphorylation on both backbone stability and the contact between dimers. It is important to note that the observed changes in spin-label mobility may not report all conformational changes, and it is also possible that very small side chain movements can be reported as large changes in spin-label mobility.

It is interesting to note that phosphorylation of positions in the head domain are usually implicated as being responsible for mediating the changes seen by phosphorylation (*46, 47*). This implies interactions between the head domain and rod 2B, and evidence exists to support this (*48, 49*). Binding affinity measurements have placed this head domain/2B interaction in the far carboxy terminus of region 2B in residues 390−411, a highly conserved region spanning the helix termination motif (HTM). Surface plasmon resonance measurements showed that this interaction is substantially lowered, and possibly eliminated, when the vimentin head domain is phosphorylated in vitro with PKA (*48*). Additional studies identified the ability of arginine but not lysine to interfere with filament assembly, and the identification of the diarginine motif in the head as critical for IF assembly offers an explanation (*49, 50*). On the basis of these data, one may speculate that interactions occur between the conserved arginines in the head domain and conserved acidic amino acids in the HTM, and Ser/Thr phosphorylation introduces negatively charged groups, eliminating this interaction.

Recent speculation that the head domain folds back along rod 1A would bring the head domain into proximity with the carboxy terminus of rod 2B in A11 tetramers, A12 tetramers, and ACN tetramers, but not in A22 tetramers (*40*). The A11 tetramer would possibly place the head domain near the amino terminus of rod 2, not near the carboxy terminus which has been identified as the binding site. Therefore, the ability of the phosphorylated vimentin head domain to disassemble IFs is possibly due to the disruption of A11, A12, or ACN tetramers. Data presented here identify the A11 tetramer as the stable tetramer formed following phosphorylation. Therefore, it is suggested that phosphorylation interferes with the formation of A12 or ACN tetramers. An alternate interpretation is that the destabilization of ACN and A12 tetramers must lead to the instability of A22 tetramers; the only tetramer that survives is the most stable and first formed, the A11 tetramer.

This hypothesized series of events, however, neglects the effects of phosphorylation on the tail. However, it has been demonstrated that tailless vimentin proteins form 10 nm filaments in vitro, suggesting the tail may be functionally less important for assembly than the head domain (*43*). Deletion of the head domain has been shown to produce

dimers and tetramers of vimentin but no higher oligomers and no IFs (*41*). The identity of the tetramer was not deduced, but on the basis of our data, we would predict it is an A11 tetramer. However, subsequent experiments support the identification of the headless vimentin tetramer as an A22 tetramer (*42*). The discrepancy between our data and data reported by Mucke et al. is likely due to the absence of the entire head domain. Transfection experiments reveal that the tail domain does have an important role in IF formation, generally summarized as stabilizing the already assembled IF. Thus, the requirement of the head domain for IF assembly coupled with our characterization of phosphorylation-induced disassembly of vimentin reveals a general assembly program whereby A11 tetramers form first followed by A22 tetramers which are most likely stabilized by additional protein contacts resulting from an A12 alignment. This structure could possibly repeat in a circular pattern to form a ULF as described by Herrmann, with final assembly of filaments the result of relatively few new protein interactions (*40*).

REFERENCES

1. Hesse, M., Magin, T. M., and Weber, K. (2001) Genes for intermediate filament proteins and the draft sequence of the human genome: novel keratin genes and a surprisingly high number of pseudogenes related to keratin genes 8 and 18. *J. Cell Sci. 114*, 2569–2575.
2. Albers, K., and Fuchs, E. (1992) The molecular biology of intermediate filament proteins. *Int. Rev. Cytol. 134*, 243–279.
3. Hanukoglu, I., and Fuchs, E. (1983) The cDNA sequence of a Type II cytoskeletal keratin reveals constant and variable structural domains among keratins. *Cell 33*, 915–924.
4. Steinert, P. M., Steven, A. C., and Roop, D. R. (1985) The molecular biology of intermediate filaments. *Cell 42*, 411–420.
5. Conway, J., and Parry, D. D. (1988) Intermediate filament structure 3. *Int. J. Biol. Macromol.* 10.
6. Fuchs, E., and Weber, K. (1994) Intermediate filaments: structure, dynamics, function, and disease. *Annu. Rev. Biochem. 63*, 345–382.
7. Kim, S., and Coulombe, P. A. (2007) Intermediate filament scaffolds fulfill mechanical, organizational, and signaling functions in the cytoplasm. *Genes Dev. 21*, 1581–1597.
8. Coulombe, P. A., and Omary, M. B. (2002) "Hard" and "soft" principles defining the structure, function and regulation of keratin intermediate filaments. *Curr. Opin. Cell Biol. 14*, 110–122.
9. Celis, J. E., Larsen, P. M., Fey, S. J., and Celis, A. (1983) Phosphorylation of keratin and vimentin polypeptides in normal and transformed mitotic human epithelial amnion cells: behavior of keratin and vimentin filaments during mitosis. *J. Cell Biol. 97*, 1429–1434.
10. Evans, R. M., and Fink, L. M. (1982) An alteration in the phosphorylation of vimentin-type intermediate filaments is associated with mitosis in cultured mammalian cells. *Cell 29*, 43–52.
11. Inagaki, M., Nishi, Y., Nishizawa, K., Matsuyama, M., and Sato, C. (1987) Site-specific phosphorylation induces disassembly of vimentin filaments in vitro. *Nature 328*, 649–652.
12. Omary, M. B., Ku, N. O., Tao, G. Z., Toivola, D. M., and Liao, J. (2006) "Heads and tails" of intermediate filament phosphorylation: multiple sites and functional insights. *Trends Biochem. Sci. 31*, 383–394.
13. Ku, N. O., and Omary, M. B. (2000) Keratins turn over by ubiquitination in a phosphorylation-modulated fashion. *J. Cell Biol. 149*, 547–552.
14. Omary, M. B., Ku, N.-O., Liao, J., and Price, D. (1998) Keratin modifications and solubility properties in epithelial cells and in vitro, in *Intermediate Filaments* (Herrmann, H., and Harris, J. R., Eds.) pp 105−140, Plenum, New York, NY.
15. Zhou, Q., Cadrin, M., Herrmann, H., Chen, C. H., Chalkley, R. J., Burlingame, A. L., and Omary, M. B. (2006) Keratin 20 serine 13 phosphorylation is a stress and intestinal goblet cell marker. *J. Biol. Chem. 281*, 16453–16461.
16. Ku, N. O., Liao, J., Chou, C. F., and Omary, M. B. (1996) Implications of intermediate filament protein phosphorylation. *Cancer Metastasis Rev. 15*, 429–444.
17. Omary, M. B., Ku, N. O., Liao, J., and Price, D. (1998) Keratin modifications and solubility properties in epithelial cells and in vitro. *Subcell. Biochem. 31*, 105–140.
18. Strelkov, S. V., Herrmann, H., Geisler, N., Lustig, A., Ivaninskii, S., Zimbelmann, R., Burkhard, P., and Aebi, U. (2001) Divide-and-conquer crystallographic approach towards an atomic structure of intermediate filaments. *J. Mol. Biol. 306*, 773–781.
19. Strelkov, S. V., Herrmann, H., Geisler, N., Wedig, T., Zimbelmann, R., Aebi, U., and Burkhard, P. (2002) Conserved segments 1A and 2B of the intermediate filament dimer: their atomic structures and role in filament assembly. *EMBO J. 21*, 1255–1266.
20. Eriksson, J. E., He, T., Trejo-Skalli, A. V., Harmala-Brasken, A. S., Hellman, J., Chou, Y. H., and Goldman, R. D. (2004) Specific in vivo phosphorylation sites determine the assembly dynamics of vimentin intermediate filaments. *J. Cell Sci. 117*, 919–932.
21. Soellner, P., Quinlan, R. A., and Franke, W. W. (1985) Identification of a distinct soluble subunit of an intermediate filament protein: tetrameric vimentin from living cells. *Proc. Natl. Acad. Sci. U.S.A. 82*, 7929–7933.
22. Tao, G. Z., Nakamichi, I., Ku, N. O., Wang, J., Frolkis, M., Gong, X., Zhu, W., Pytela, R., and Omary, M. B. (2006) Bispecific and human disease-related anti-keratin rabbit monoclonal antibodies. *Exp. Cell Res. 312*, 411–422.
23. Evans, R. M. (1988) The intermediate-filament proteins vimentin and desmin are phosphorylated in specific domains. *Eur. J. Cell Biol. 46*, 152–160.
24. Inagaki, M., Gonda, Y., Nishizawa, K., Kitamura, S., Sato, C., Ando, S., Tanabe, K., Kikuchi, K., Tsuiki, S., and Nishi, Y. (1990) Phosphorylation sites linked to glial filament disassembly in vitro locate in a non-α-helical head domain. *J. Biol. Chem. 265*, 4722–4729.
25. Avram, D., Romijn, E. P., Pap, E. H., Heck, A. J., and Wirtz, K. W. (2004) Identification of proteins in activated human neutrophils susceptible to tyrosyl radical attack. A proteomic study using a tyrosylating fluorophore. *Proteomics 4*, 2397–2407.
26. Ando, S., Tanabe, K., Gonda, Y., Sato, C., and Inagaki, M. (1989) Domain- and sequence-specific phosphorylation of vimentin induces disassembly of the filament structure. *Biochemistry 28*, 2974–2979.
27. Geisler, N., Hatzfeld, M., and Weber, K. (1989) Phosphorylation in vitro of vimentin by protein kinases A and C is restricted to the head domain. Identification of the phosphoserine sites and their influence on filament formation. *Eur. J. Biochem. 183*, 441–447.
28. Cheng, T. J., Tseng, Y. F., Chang, W. M., Chang, M. D., and Lai, Y. K. (2003) Retaining of the assembly capability of vimentin phosphorylated by mitogen-activated protein kinase-activated protein kinase-2. *J. Cell. Biochem. 89*, 589–602.
29. Budamagunta, M., Hess, J., Fitzgerald, P., and Voss, J. (2007) Describing the structure and assembly of protein filaments by EPR spectroscopy of spin-labeled side chains. *Cell Biochem. Biophys. 48*, 45–53.
30. Hess, J., Budamagunta, M. S., R, S., Voss, J., and Fitzgerald, P. (2005) Characterization of the linker region of vimentin using site directed spin labeling and electron paramagnetic resonance, J. Biol. Chem. (submitted for publication).
31. Hess, J. F., Budamagunta, M. S., FitzGerald, P. G., and Voss, J. C. (2005) Characterization of structural changes in vimentin bearing an epidermolysis bullosa simplex-like mutation using site-directed spin labeling and electron paramagnetic resonance. *J. Biol. Chem. 280*, 2141–2146.
32. Hess, J. F., Budamagunta, M. S., Voss, J. C., and FitzGerald, P. G. (2004) Structural characterization of human vimentin rod 1 and the sequencing of assembly steps in intermediate filament formation in vitro using site-directed spin labeling and electron paramagnetic resonance. *J. Biol. Chem. 279*, 44841–44846.
33. Hess, J. F., Voss, J. C., and FitzGerald, P. G. (2002) Real-time observation of coiled-coil domains and subunit assembly in intermediate filaments. *J. Biol. Chem. 277*, 35516–35522.
34. Parry, D. A., Marekov, L. N., and Steinert, P. M. (2001) Subfilamentous protofibril structures in fibrous proteins: cross-linking evidence for protofibrils in intermediate filaments. *J. Biol. Chem. 276*, 39253–39258.
35. Steinert, P. M., Marekov, L. N., and Parry, D. A. (1993) Diversity of intermediate filament structure. Evidence that the alignment of coiled-coil molecules in vimentin is different from that in keratin intermediate filaments. *J. Biol. Chem. 268*, 24916–24925.

36. Shevchenko, A., Wilm, M., Vorm, O., and Mann, M. (1996) Mass spectrometric sequencing of proteins silver-stained polyacrylamide gels. *Anal. Chem. 68*, 850–858.
37. Sen, K. I., Logan, T. M., and Fajer, P. G. (2007) Protein dynamics and monomer-monomer interactions in AntR activation by electron paramagnetic resonance and double electron-electron resonance. *Biochemistry 46*, 11639–11649.
38. Kokorin, A. I., Zamaraev, K. I., Grigorian, G. L., Ivanov, V. P., and Rozantsev, E. G. (1972) Measurement of the distance between paramagnetic centers in solid solutions of nitrosyl radicals, biradicals and spin-labelled proteins. *Biofizika 17*, 34–41.
39. Likhtenshtein, G. I. (1993) *Biophysical labeling methods in molecular biology*, Cambridge University Press, New York.
40. Herrmann, H., and Aebi, U. (2004) Intermediate filaments: molecular structure, assembly mechanism, and integration into functionally distinct intracellular Scaffolds. *Annu. Rev. Biochem. 73*, 749–789.
41. Herrmann, H., Haner, M., Brettel, M., Muller, S. A., Goldie, K. N., Fedtke, B., Lustig, A., Franke, W. W., and Aebi, U. (1996) Structure and assembly properties of the intermediate filament protein vimentin: the role of its head, rod and tail domains. *J. Mol. Biol. 264*, 933–953.
42. Mucke, N., Wedig, T., Burer, A., Marekov, L. N., Steinert, P. M., Langowski, J., Aebi, U., and Herrmann, H. (2004) Molecular and biophysical characterization of assembly-starter units of human vimentin. *J. Mol. Biol. 340*, 97–114.
43. McCormick, M. B., Kouklis, P., Syder, A., and Fuchs, E. (1993) The roles of the rod end and the tail in vimentin IF assembly and IF network formation. *J. Cell Biol. 122*, 395–407.
44. Vikstrom, K. L., Lim, S. S., Goldman, R. D., and Borisy, G. G. (1992) Steady state dynamics of intermediate filament networks. *J. Cell Biol. 118*, 121–129.
45. Columbus, L., and Hubbell, W. L. (2002) A new spin on protein dynamics. *Trends Biochem. Sci. 27*, 288–295.
46. Geisler, N., and Weber, K. (1988) Phosphorylation of desmin in vitro inhibits formation of intermediate filaments; identification of three kinase A sites in the aminoterminal head domain. *EMBO J. 7*, 15–20.
47. Martys, J. L., Ho, C. L., Liem, R. K., and Gundersen, G. G. (1999) Intermediate filaments in motion: observations of intermediate filaments in cells using green fluorescent protein-vimentin. *Mol. Biol. Cell 10*, 1289–1295.
48. Gohara, R., Tang, D., Inada, H., Inagaki, M., Takasaki, Y., and Ando, S. (2001) Phosphorylation of vimentin head domain inhibits interaction with the carboxyl-terminal end of α-helical rod domain studied by surface plasmon resonance measurements. *FEBS Lett. 489*, 182–186.
49. Traub, P., Scherbarth, A., Wiegers, W., and Shoeman, R. L. (1992) Salt-stable interaction of the amino-terminal head region of vimentin with the α-helical rod domain of cytoplasmic intermediate filament proteins and its relevance to protofilament structure and filament formation and stability. *J. Cell. Sci. 101*, 363–381.
50. Herrmann, H., Hofmann, I., and Franke, W. W. (1992) Identification of a nonapeptide motif in the vimentin head domain involved in intermediate filament assembly. *J. Mol. Biol. 223*, 637–650.

BI801137M